The American Journal of Pathology, Vol. 178, No. 6, June 2011
Published by Elsevier Inc. on behalf of the
American Society for Investigative Pathology.
DOI: 10.1016/j.ajpath.2011.02.038

Immunopathology and Infectious Diseases

Role of p47phox in Antigen-Presenting Cell-Mediated Regulation of Humoral Immunity in Mice

Sam Vasilevsky,* Qi Liu,* Sherry M. Koontz,* Robin Kastenmayer,† Katherine Shea,† and Sharon H. Jackson*

From the Molecular Trafficking Unit, Laboratory of Host Defenses, and the Infectious Disease Pathogenesis Section,† Comparative Medicine Branch, National Institute of Allergy and Infectious Diseases, National Institutes of Health, Bethesda, Maryland*

Microbial-induced inflammation is important for eliciting humoral immunity. Genetic defects of NADPH oxidase 2–based proteins interrupt phagocyte superoxide generation and are the basis for the human immunodeficiency chronic granulomatous disease (CGD). Hyperinflammation is also a significant clinical manifestation of CGD. Herein, we evaluated humoral immunity in the phagocyte oxidase p47^{phox}-deficient model of CGD and found that UV-inactivated *Streptococcus pneumoniae* and *Listeria monocytogenes* (*Lm*) elicited higher specific antibody (Ab) titers in p47$^{phox-/-}$ mice than wild-type (WT) mice. Both organisms elicited robust and distinct antigen-presenting cell maturation phenotypes, including IL-12 hypersecretion, and higher major histocompatibility complex II and costimulatory protein expression in *Lm*-stimulated p47$^{phox-/-}$ dendritic cells (DCs) relative to WT DCs. Furthermore, p47$^{phox-/-}$ DCs pulsed with *Lm* and adoptively transferred into naïve WT mice elicited Ab titers, whereas *Lm*-pulsed WT DCs did not elicit these titers. The observed robust p47$^{phox-/-}$ mouse humoral response was recapitulated with live *Lm* and sustained *in vivo* in p47$^{phox-/-}$ mice. Notably, anti–serum samples from p47$^{phox-/-}$ mice that survived secondary *Lm* infection were protective in WT and p47$^{phox-/-}$ mice that were rechallenged with secondary lethal *Lm* infection. These findings demonstrate a novel benefit of NADPH oxidase 2 deficiency (ie, dependent inflammation in antigen-presenting cell–mediated humoral immunity) and that anti-*Lm* Ab can be protective in an immunodeficient CGD host. ***(Am J Pathol 2011, 178: 2774–2782; DOI: 10.1016/j.ajpath.2011.02.038)***

Antigen-presenting cells (APCs), such as dendritic cells (DCs) and macrophages, are important cellular mediators of inflammation. APCs also bridge innate and humoral immunity to combat microbial infection. Bacteria induce APC maturation. In turn, mature APCs instruct adaptive immunity by presenting bacteria-derived peptides, along with costimulatory signals, to T cells and secreting inflammatory cytokines that drive T-cell activation and consequent T-cell–mediated and/or humoral immunity.

Both *Listeria monocytogenes (Lm*), a facultative intracellular bacterium, and *Streptococcus pneumoniae (Pn*), an anaerobic extracellular bacterium, have been used to study the fundamental components of innate and adaptive immunity.[1–3] *Lm* and *Pn* each elicit strong APC-mediated inflammatory and cellular responses that are important for initiating protective immune responses.

Pn elicits antigen-specific antibody (Ab) production and anti-*Pn* humoral immunity.[3] In contrast, early *Lm* research[4] indicated that *Lm*-induced Ab production was not specific for *Lm* resistance, and experimental evidence[1,2] showed that T-cell–mediated immunity is most critical for eliminating *Lm*. However, subsequent studies[5,6] have shown that humoral immunity can play a significant role in the elimination of *Listeria* infection.

The local oxidative environment, reactive oxygen species (ROS), and free radical responses are widely postulated to promote inflammation as part of the adaptive response to restoring tissue homeostasis after acute infection and tissue injury. However, recent observations that phagocytes, and nonphagocytic cells, generate ROS as they orchestrate adaptive immune responses raise questions about the source and relative role of ROS in modulating inflammatory responses that are important for eliciting humoral immunity.[7,8] Patients with chronic gran-

Supported by the Division of Intramural Research of the National Institutes of Health/National Institute of Allergy and Infectious Diseases and partially supported by the National Institutes of Health/National Center on Minority Health and Health Disparities.

Accepted for publication February 8, 2011.

Address reprint request to Sharon H. Jackson, M.D., Laboratory of Host Defenses, National Institute of Allergy and Infectious Diseases, NIH, CRC Bldg 5-West Labs, 10 Center Dr, MSC 1456, Room 5-3942, Bethesda, MD 20892-1456. E-mail: sjackson@niaid.nih.gov.

ulomatous disease (CGD) have heterogeneous genetic defects of phagocytic oxidase NADPH oxidase 2 (Nox2)–based proteins and an absent or reduced phagocyte respiratory burst.[9–12] CGD is a multifaceted clinical disease that manifests clinically as life-threatening bacterial and fungal infections.[9,13] Interestingly, noninfectious hyperinflammation is also a common occurrence in patients with CGD.[14] Because one of the clinical manifestations of CGD is increased inflammation, we investigated the ability of $p47^{phox}$ (*Ncf1*)–deficient ($p47^{phox-/-}$) APCs to secrete cytokines and up-regulate receptors important for initiating humoral immunity against *Lm* and *Pn*. We demonstrate that *Pn* and *Lm* stimulation leads to dissimilar $p47^{phox-/-}$ DC maturation. We also show that, although *Pn* predictably induces humoral immunity, including memory Ab production in $p47^{phox-/-}$ mice, anti-*Pn* humoral immunity is enhanced in $p47^{phox-/-}$ mice compared with wild-type (WT) control mice. Interestingly, we found that *Lm* similarly elicits enhanced and protective humoral immunity in $p47^{phox-/-}$ mice.

Materials and Methods

Mice

Nox $p47^{phox}$-deficient ($p47^{phox-/-}$) mice have been described.[15,16] Congenic $p47^{phox-/-}$ mice on a C57BL/6NTac background were generated by backcrossing over 10 generations with WT C57BL/6NTac. $gp91^{phox-/-}$/$Nox2^{-/-}$ B6.129S6-*Cybb*^{tm1Din}/J mice[17] were obtained from The Jackson Laboratory (Bar Harbor, ME). Animal care was provided in accordance with Institutional Animal Care and Use Committee procedures, approved by the National Institute of Allergy and Infectious Diseases, NIH (Bethesda, MD). All mice used were between the ages of 3 and 6 weeks.

Preparation of Pn *Type 2 (R36A) and* Lm

Frozen stocks of nonencapsulated variant (strain R36A) of virulent *Pn* capsular type 2 (strain D39) were thawed and subcultured on BBL agar plates (VWR International, West Chester, PA). Similarly, recombinant *Lm* strain 10403S expressing ovalbumin; a gift from Dr. Hao Chen[18] (University of Pennsylvania School of Medicine, Philadelphia, PA) was subcultured on Difco Brain Heart Infusion Agar (BD, Franklin Lakes, NJ). Isolated colonies were collected and UV inactivated (UVi) (UV Stratalinker 1880; Artisan Scientific, Champagne, IL) at 1000 mJ for 1 hour. Sterility was confirmed by subculture on blood agar plates for *Pn* and Brain Heart Infusion Agar for *Lm*. After extensive washings, the bacterial suspensions were adjusted with PBS to provide an OD of 0.6, which corresponded to 10^9 colony-forming units (CFUs)/mL of *Pn*; and 0.1, which corresponded to 10^8 CFUs/mL of *Lm*. Bacteria were then divided at 10^{10} CFUs/mL and frozen at -80°C until their use.

Preparation of Bone Marrow–Derived Dendritic Cells

Bone marrow–derived DCs (BMDCs) were prepared as previously described.[19] Briefly, bone marrow was flushed with PBS, resuspended in 1 mL ACK Lysing Buffer (Bio-Whittaker, Walkersville, MD), and incubated at room temperature for 5 minutes to eliminate red cells. The single-cell suspension was filtered through a 40-μm cell strainer (BD Falcon/BD Biosciences, San Jose, CA), resuspended at a density of 1.25×10^6 cells/mL (24-well plates) in RPMI 1640 plus 5% fetal bovine serum, 10,000 IU penicillin, 10 mg/mL streptomycin, 1 mmol/L sodium pyruvate, 2 mmol/L L-glutamine, 0.1 mmol/L nonessential amino acids, and 25 mmol/L HEPES (culture medium), supplemented with 10 ng/mL murine recombinant granulocyte macrophage colony-stimulating factor (M-CSF) (Sigma-Aldrich, St. Louis, MO). After 7 days of culture, nonadherent cells were harvested.

Preparation of Bone Marrow–Derived Macrophages

Bone marrow–derived macrophages (BMMs) were obtained using a similar approach as used for BMDCs, with slight modifications. Bone marrow cells were cultured at 1×10^6 cells/mL in cell culture medium supplemented with 10 ng/mL murine M-CSF (Sigma-Aldrich). Cells were plated in six-well plates in a volume of 4 to 5 mL per well. On days 3 and 5, three-fourths culture medium was removed; and fresh culture medium was added. On day 7, BMMs were harvested by washing plates with sterile PBS to remove nonadherent cells. Cells were detached from the plate as previously described.[19] Briefly, 2 mL of detachment buffer (4 mg/mL lidocaine, 5 mmol/L EDTA, and PBS) was added for 3 to 5 minutes. After incubation, detachment buffer was pipetted until the adherent cells detached.

Reagents

Recombinant pneumococcal surface protein A (PspA; family 1, sero clade 2) was provided by Clifford M. Snapper (Uniformed Services University of the Health Sciences, Bethesda). Purified listeriolysin-O (LLO) was purchased from Abcam (Cambridge, MA).

Histopathological and Immunohistochemical Features

A necropsy of all mice was performed at the ages noted. All tissues were examined grossly, and most were fixed in 10% neutral-buffered formalin, embedded in paraffin, and sectioned. Slides containing formalin-fixed, paraffin-embedded tissue sections (3 to 4 μm) were deparaffinized in xylene and rehydrated by processing them through alcohols. Pretreatment of tissues before incubation with the *Listeria* primary Ab consisted of bleaching with Peroxidazed 1 (Biocare Medical, Concord, CA) for 5 minutes, digesting with proteinase K (Dako, Carpentaria,

CA) for 5 minutes, and pageing with Background Sniper (Biocare Medical) for 10 minutes. Sections were incubated with a goat polyclonal Ab against *Listeria* (KPL, Gaithersburg, MD) for 60 minutes at a dilution of 1:1500. The bound Ab was detected using a goat polymer detection system (Biocare Medical) and Vulcan Fast Red chromogen (Biocare Medical). Sections were counterstained with CAT hematoxylin (Biocare Medical), air dried, and mounted using Permount mounting medium (Fisher Scientific, Pittsburgh, PA). Negative controls included replacing the primary Ab with normal goat serum at a comparable protein concentration and testing noninfected tissues with the primary Ab. Slides were imaged using Aperio ScanScope software (Aperio Technologies Inc., Vista, CA).

Flow Cytometric Analysis

All steps were performed on ice. Fc receptors were pageed with 10 μg/mL purified rat anti-mouse CD16/CD32 mouse Fc page (clone 2.4G2). Cells were stained for 30 minutes with fluorescein isothiocyanate–mouse IgG2a and κ anti-mouse major histocompatibility complex (MHC) class II^b (clone AF6-120.1), phosphatidylethanolamine-mouse IgG2a and κ anti-mouse CD40 (clone 3/23), phosphatidylethanolamine-mouse IgG2a and κ anti-mouse CD86 (clone GL1), and Armenian hamster IgG2 and κ anti-mouse CD80 (clone 16-10A1). All monoclonal antibodies were purchased from BD Pharmingen (Franklin Lakes, NJ). Irrelevant isotype- and species-matched monoclonal antibodies (Abs) were used as staining controls. Cells were analyzed on a BD FacsCanto flow cytometer.

In Vitro *Incubation of BMDCs and BMMs with Bacteria*

BMDCs, cultured in granulocyte M-CSF, and BMMs, cultured in M-CSF, were pulsed *in vitro* with UVi *Pn* (10^8 CFUs) or UVi *Lm* (10^8 CFUs) overnight. IL-6, IL-12, and tumor necrosis factor (TNF)-α were measured from supernatant by sandwich enzyme-linked immunosorbent assay (ELISA).

In Vivo *Bacterial Challenge*

WT, p47$^{phox-/-}$, and/or Nox2$^{-/-}$ mice were immunized by i.p. injection with 2×10^8 CFUs of UVi *Pn* or *Lm* on day 0; on day 14, a secondary challenge of UVi bacteria was given to assess the potential generation of memory. Serum was harvested 7, 14 (before rechallenge), and 21 days after bacterial challenge. For live *Lm* infection, WT and p47$^{phox-/-}$ mice were infected i.v. with 5×10^4 CFUs (0.1 LD50) of *Lm*.

Measurement of Serum Ig Titers

ELISA plates (Immunolon 4) were coated with 5 μg/mL (50 μL/well) PspA, 3 μg/mL (50 μL/well) LLO, and 3 μg/mL (50 μL/well) UVi *Pn* (10^7 CFUs/well) or UVi *Lm* (10^7 CFUs/well) in PBS overnight at 4°C. Plates were pageed with PBS plus 1% bovine serum albumin (BSA) for 30 minutes at 37°C and washed three times with PBS plus 0.1% Tween 20. Threefold dilutions of serum samples, starting at a 1:50 serum dilution, in PBS plus 0.05% Tween 20 were then added and left overnight at 4°C. Plates were washed three times with PBS plus 0.1% Tween 20. Alkaline phosphatase–conjugated polyclonal goat anti-mouse IgM or IgG Abs (200 ng/mL final concentration in PBS plus 0.05% Tween 20) were then added, and plates were incubated for 37°C for 1 hour. Plates were washed five times with PBS plus 0.1% Tween 20. Substrate (*p*-nitrophenyl phosphate, disodium) at 1 mg/mL in TM buffer [1 mol/L Tris plus 0.3 mmol/L $MgCl_2$ (pH 9.8)] was then added for 30 minutes at room temperature for color development. Color was read at an absorbance of 405 nm.

Measurement of Cytokine Concentrations in Culture Supernatant by ELISA

Concentrations of specific cytokines released into the medium of cell cultures were measured using optimized standard sandwich ELISA. ELISA (Immunolon 4) plates were coated with IL-6 (2 μg/mL), IL-12 (6 μg/mL), and TNF-α (10 μg/mL) capture Ab in PBS overnight at 4°C. Plates were pageed with PBS plus 1% BSA for 30 minutes at 37°C and washed three times with PBS plus 0.1% Tween 20. Twofold dilutions of supernatant samples and standards, including recombinant (r) IL-6 (4 ng/mL), rIL-12 (8 ng/mL), or rTNF-α (8 ng/mL) in PBS plus 0.05% Tween 20, were then added and left overnight at 4°C. Plates were washed three times with PBS plus 0.1% Tween 20. Secondary IL-6 (1 μg/mL), IL-12 (1 μg/mL), and TNF-α (1 μg/mL) antibodies with PBS plus 1% BSA were added for 1 hour at 37°C and washed three times with PBS plus 0.1% Tween 20. Streptavidin-alkaline phosphatase with PBS plus 1% BSA was added at a 1:1000 concentration for 1 hour at 37°C. Substrate (*p*-nitrophenyl phosphate, disodium; at 1 mg/mL in TM buffer [1 mol/L Tris plus 0.3 mmol/L $MgCl_2$ (pH 9.8)] was then added for 30 minutes at room temperature for color development. Color was read at an absorbance of 405 nm.

Immune Serum Transfer

Twenty WT and p47$^{phox-/-}$ mice were i.v. infected with 5×10^4 *Lm*, then were rechallenged with 5×10^6 *Lm* 28 days later. Serum was harvested from the surviving WT (n = 20) and p47$^{phox-/-}$ (n = 16) mice 6 days after reinfection and was adoptively transferred i.v. into a second set of WT and p47$^{phox-/-}$ recipients that were infected with 5×10^4 *Lm* 28 days previously. One day after immune serum transfer, WT and p47$^{phox-/-}$ mice were reinfected with 5×10^6 *Lm* and monitored for survival.

Statistics

Differences between the group means were analyzed by the Student's *t*-test (Prism 5; GraphPad Software, Inc.,

Table 1. APC Cytokine Secretion from WT and p47$^{phox-/-}$ Mice Cultured with 1 × 10^8 CFUs/mL of UVi *Pn* or *Lm* for 24 Hours *in Vitro*

	IL-6		IL-12		TNF-α	
Variable	WT	p47$^{phox-/-}$	WT	p47$^{phox-/-}$	WT	p47$^{phox-/-}$
BMDCs						
Pn	5.68 ± 0.63	10.27 ± 0.88*	1.25 ± 0.04	1.37 ± 0.06	ND	0.89 ± 0.03
Lm	24.39 ± 0.63	21.24 ± 0.88	3.12 ± 0.14	4.82 ± 0.03†	5.25 ± 0.30	3.62 ± 0.50
Medium	0.625 ± 0.03	0.646 ± 0.002	0.263 ± 0.001	0.237 ± 0.57	ND	0.393 ± 0.17
BMMs (M-CSF)						
Pn	0.75 ± 0.09	2.05 ± 0.08†	1.40 ± 0.09	4.70 ± 0.10†	ND	1.84 ± 0.09
Lm	2.81 ± 0.39	5.16 ± 0.33*	1.89 ± 0.07	6.43 ± 0.12†	1.50 ± 0.20	3.87 ± 0.14†
Medium	ND	ND	ND	ND	ND	1.42 ± 0.38

Data are given as mean ± SEM (in ng/mL). $n = 4$. Concentrations of IL-6, IL-12, and TNF-α in the culture supernatant were determined by ELISA. The limit of detection for IL-6 was <31 pg/mL; IL-12, <62 pg/mL; and TNF-α, <250 pg/mL. Data are from Vasilevsky et al.[19]

*$P = 0.04$.

†$P = 0.0004$.

ND, not detectable.

San Diego, CA). $P \leq 0.05$ was considered statistically significant.

Results

Lm *and* Pn *Elicit Distinct Maturation Phenotypes in p47$^{phox-/-}$ and WT APCs*

For initial investigations, we used UVi *Lm* or *Pn* to compare proinflammatory cytokine induction in WT and p47$^{phox-/-}$ BMMs and BMDCs propagated *in vitro*. In contrast to heat-killed inactivation, which can cause bacterial rupture, UV-irradiated bacteria are replication incompetent[20] and remain structurally intact. As illustrated in Table 1, *Pn*-pulsed p47$^{phox-/-}$ APCs hypersecrete IL-6 and TNF-α; in contrast, *Lm*-stimulated p47$^{phox-/-}$ APCs hypersecrete IL-12 relative to WT APCs. Interestingly, although *Lm*-pulsed p47$^{phox-/-}$ DCs secrete less TNF-α than WT DCs, p47$^{phox-/-}$ macrophages propagated in M-CSF secreted at least twofold more IL-6, IL-12, and TNF-α in response to both *Pn* and *Lm* relative to WT macrophages (Table 1).

Next, we compared MHCs with costimulatory molecule expression in *Lm*- and *Pn*-stimulated APCs (Table 2). After overnight culture with UVi microorganisms, p47$^{phox-/-}$ DCs expressed higher surface levels of MHC class II and CD80 in media alone and in response to *Lm* stimulation compared with WT DCs (Figure 1A). In addition, surface CD40 and CD86 is significantly up-regulated in *Lm*-stimulated p47$^{phox-/-}$ DCs relative to similarly treated WT DCs. In contrast, WT DCs expressed higher surface levels of MHC class II, CD86, and CD40 in response to *Pn* stimulation compared with p47$^{phox-/-}$ DCs (Figure 1B). WT and p47$^{phox-/-}$ macrophages propagated

Table 2. APC MFI Values

	BMDCs				BMMs			
	WT		p47$^{phox-/-}$		WT		p47$^{phox-/-}$	
Variable	gMFI	No. of cells	gMFI	No. of cells	gMFI	No. of cells	gMFI	No. of cells
MHC Class II								
Medium	72	5481	123	5749	230	3195	342	3970
Pn	123	4630	100	6976	1241	6377	1877	6590
Lm	141	4568	210	6466	958	7242	895	7418
Control	56	6521	60	7119	366	4140	343	7518
CD80								
Medium	503	4550	1033	6477	462	4955	384	5017
Pn	621	5900	1147	6383	558	5824	721	7163
Lm	511	6059	1656	5743	451	6550	582	7501
Control	130	6461	127	7843	324	8207	290	7375
CD86								
Medium	336	5590	266	6848	278	44,879	351	4280
Pn	751	6129	309	7344	439	4969	529	7198
Lm	427	4438	1035	5859	677	7490	725	7516
Control	114	5807	86	8522	245	4140	232	7375
CD40								
Medium	208	5764	130	6673	821	3586	446	4513
Pn	379	6122	255	7494	2142	6699	2028	7040
Lm	355	4435	755	6069	2592	7353	1374	6979
Control	114	5807	127	7843	73	7375	75	7375

APCs from WT and p47$^{phox-/-}$ mice were cultured with 1 10^8 CFUs/mL of UVi *Pn* or *Lm* for 24 hours *in vitro*.

gMFI, geometric mean fluorescence intensity.

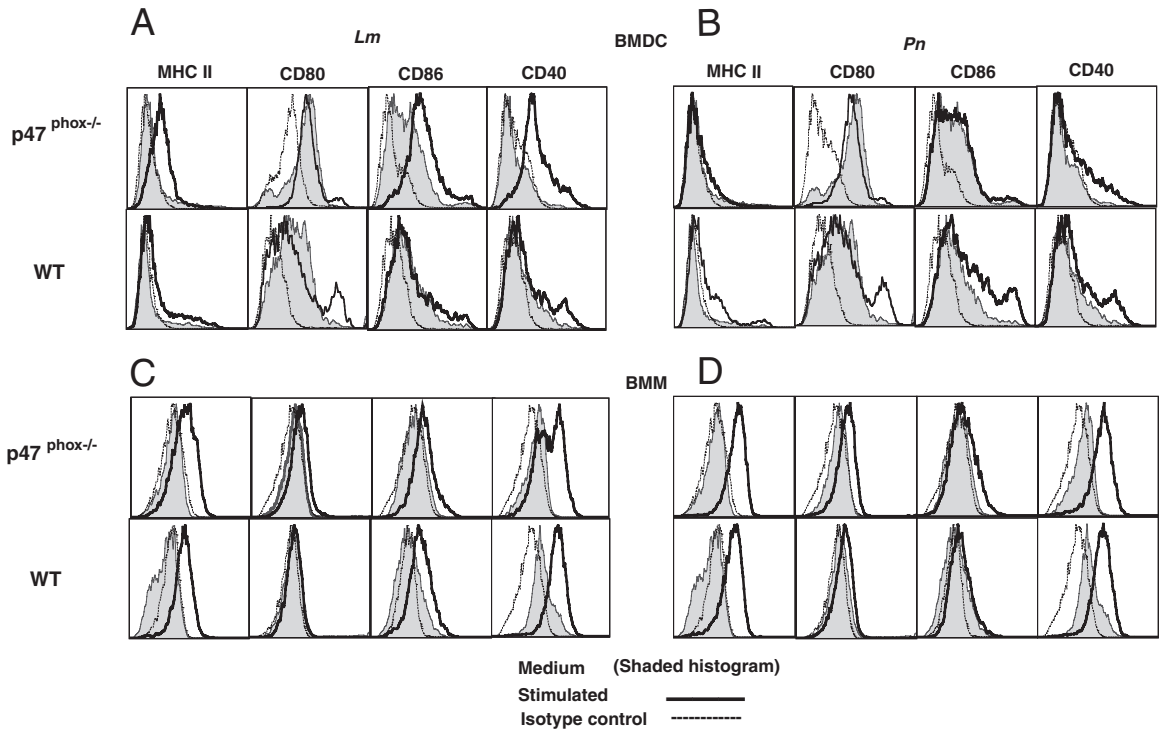

Figure 1. *Pn*- and *Lm*-induced maturation of p47$^{phox-/-}$ and WT APCs *in vitro*. WT and p47$^{phox-/-}$ BMDCs (**A** and **B**) and BMMs (**C** and **D**) (1×10^6 cells/mL) were stained with fluorochrome-conjugated monoclonal Abs specific for the indicated cell surface proteins after 24 hours in culture in medium alone or in the presence of UVi *Pn* or *Lm* (1×10^9 CFUs/mL) and analyzed by flow cytometry. Results are representative of two independent experiments with pooled cells from three to four of each genotype per experiment.

in M-CSF and pulsed with *Lm* or *Pn* similarly up-regulated MHC class II, CD80, CD86, and CD40 (Figure 1, C and D). Thus, in addition to finding that p47^{phox} differentially regulates proinflammatory cytokine secretion in *Pn*- and *Lm*-stimulated APCs, these observations show that *Pn* and *Lm* induce distinct maturation immunophenotypes in p47$^{phox-/-}$ and WT APCs. Notably, only *Lm*-pulsed p47$^{phox-/-}$ DCs expressed higher levels of MHC class II, CD80, CD86, and CD40 compared with WT, suggesting a role for p47^{phox} in DC antigen presentation.

*p47$^{phox-/-}$ DC–Mediated Regulation of Anti-*Lm *Humoral Immunity*

Although *Pn*-elicited humoral immunity in mice is well characterized,[3,21] few investigations[5,6] have shown a benefit for *Lm*-induced humoral immunity and Ab production. Next, to clarify whether p47^{phox} deficiency affected anti-*Lm* Ab production, we used ELISA to compare specific Ab titers for intact bacteria and *Pn* and *Lm* virulence factors, PspA and LLO, respectively, after UVi *Pn* or *Lm* challenge. Although LLO is a heat-liable protein,[22] we exploited our UVi challenge model to examine this parameter. For these investigations, we immunized p47$^{phox-/-}$ and WT mice with UVi bacteria on day 0; on day 14, a secondary challenge of UVi bacteria was given to assess the generation of memory Ab production. As illustrated in Figure 2A, *Pn* predictably induced potent Ab production in both WT and p47$^{phox-/-}$ mice. However, the p47$^{phox-/-}$ anti-*Pn* IgM titers were twofold higher than WT 7 and 14 days after UVi *Pn* challenge. In addition, p47$^{phox-/-}$ anti-*Pn* IgG titers were threefold higher on day 7 before rechallenge and twofold higher than WT after UVi *Pn* rechallenge (Figure 2A, day 21). Similarly, p47$^{phox-/-}$ mice had higher IgM and IgG isotype PspA-specific titers than WT mice after UVi *Pn* challenge (Figure 2C). Notably, serum from UVi-*Lm*–challenged p47$^{phox-/-}$ mice also exhibited increased anti-*Lm* IgM (twofold to threefold higher on days 7 and 14) and IgG (33-fold higher on day 14 and 15-fold higher on day 21) titers relative to WT mice (Figure 2B). Moreover, p47$^{phox-/-}$ anti-LLO IgM titers were elevated 11-fold on day 21 and anti-LLO IgG titers were elevated twofold higher than WT on day 14; serum anti-LLO IgG titers in WT and p47$^{phox-/-}$ mice were similar on day 21 after a secondary UVi *Lm* boost on day 14 (Figure 2C). Collectively, these results demonstrate that humoral immunity is enhanced in inflammation-prone p47$^{phox-/-}$ mice and thereby reveal a complex and unforeseen benefit of phagocyte oxidase deficiency for enhancing anti-*Pn* and *Lm* humoral immunity.

Previous investigations[23,24] showed that, although gp91^{phox}-deficient (Nox2$^{-/-}$) mice have increased susceptibility to *Lm* infection and that Nox2$^{-/-}$ macrophages cannot kill virulent *Lm*, primary *Lm* infection is not fatal in p47$^{phox-/-}$ mice.[25] Thus, to discern the role of p47^{phox} independently or as part of the multicomponent phagocytic Nox in *Lm*-elicited humoral immunity, we examined *Lm*-induced Ab production in Nox2$^{-/-}$ catalytic subunit mice. As shown in Figure 2B, compared with p47$^{phox-/-}$

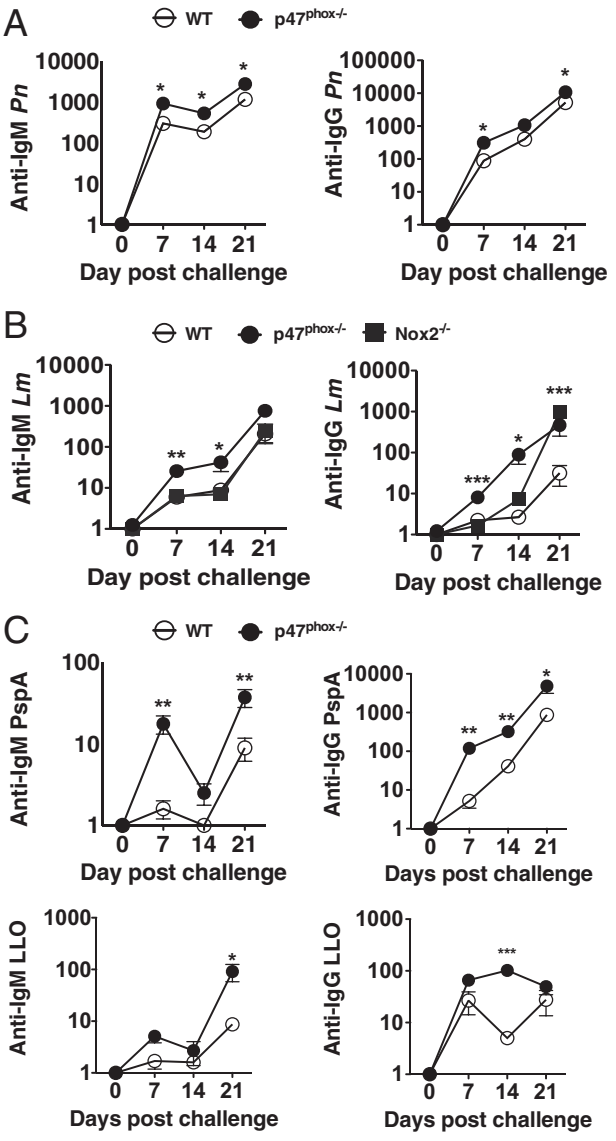

Figure 2. Ab production in response to UVi *Pn* and *Lm* challenge. WT, p47$^{phox-/-}$, and Nox2$^{-/-}$ mice were immunized by i.p. injection with 2×10^8 CFUs of UVi *Pn* or *Lm* on days 0 and 14 before serum collection. Serum was harvested on the indicated days. Serum titers for IgG and IgM specific for whole *Pn* (**A**), *Lm* (**B**), and PspA and LLO (**C**) were determined by ELISA. Absorbance values (Titer-1) represent the mean ± SEM. $^*P \leq 0.05$, $^{**}P \leq 0.005$, and $^{***}P \leq 0.0005$. Results are representative of two individual experiments with five of each genotype per experiment.

mice, anti-*Lm* IgM-specific titers were not elevated from *Lm*-challenged Nox2$^{-/-}$ mice. However, anti–*Lm*-specific IgG titers were elevated 2.5-fold on day 14 in Nox2$^{-/-}$ mice compared with *Lm*-challenged WT mice and twofold and 31-fold compared with p47$^{phox-/-}$ and WT mice, respectively, on day 21 after a secondary *Lm* boost on day 14 (Figure 2B). These data show that, although the kinetics of anti–*Lm*-specific IgG induction are different in Nox2$^{-/-}$ and p47$^{phox-/-}$ mice, *Lm* challenge elicits an equally robust recall IgG Ab response in Nox2$^{-/-}$ mice as in p47$^{phox-/-}$ mice, therefore indicating that Nox2 enzymatic activity is important for controlling *Lm*-elicited Ab production.

These observations lead us to question the relevance of the observed enhanced *Lm*-induced p47$^{phox-/-}$ DC maturation phenotype to the robust UVi *Lm*-elicited humoral response in p47$^{phox-/-}$ mice and whether the anti-*Lm* humoral immune response may be protective in p47$^{phox-/-}$ mice. Therefore, to further investigate these parameters, we adoptively transferred 1×10^6 *Lm*-pulsed p47$^{phox-/-}$ and WT BMDCs into naïve WT recipient mice. As controls, unpulsed p47$^{phox-/-}$ and WT DCs were also transferred into a separate group of WT recipients. There was no difference in anti-*Lm* IgM or IgG titers in WT recipients of *Lm*-pulsed or unpulsed control DCs 7 and 14 days after DC transfer (data not shown). In contrast, there was a threefold difference in anti-*Lm* IgM titers in WT mice that received *Lm*-pulsed p47$^{phox-/-}$ DCs compared with recipients that received unpulsed p47$^{phox-/-}$ DCs 7 and 14 days after DC transfer (Figure 3). However, there was no difference in anti-*Lm* IgG titers in these mice. To assess whether the adoptively transferred p47$^{phox-/-}$ DCs could prime for a recall response, we challenged the DC recipients with UVi *Lm* after serum harvest on day 14. As shown in Figure 3, there was a 14-fold increase on day 21 in anti-*Lm* IgG titers of recipients of *Lm*-pulsed p47$^{phox-/-}$ DCs compared with day 14 titers. Thus, *Lm*-pulsed p47$^{phox-/-}$ DCs elicit similar IgM titers to those seen in WT and p47$^{phox-/-}$ mice challenged with UVi (Figure 2) and are primed for anti-*Lm* IgG recall humoral immunity.

Immune Serum from Lm-*Infected p47$^{phox-/-}$ Mice Is Protective against Secondary* Lm *Challenge*

Next, we immunized p47$^{phox-/-}$ and WT mice with a sublethal dose of live *Lm* and collected serum after 7, 14, and 120 days to determine whether live *Lm* infection would also elicit higher Ab production in p47$^{phox-/-}$ mice. Histological examination results of spleens from

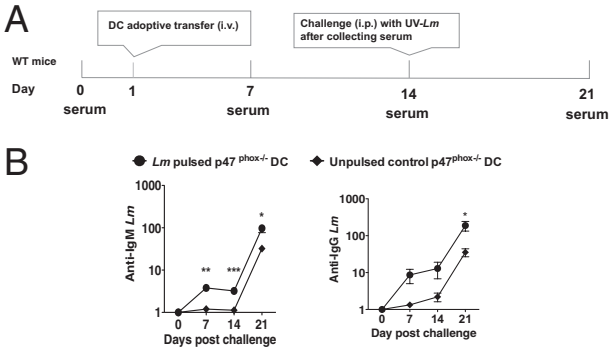

Figure 3. p47^{phox} in DCs is critical for IgM and IgG Abs in response to *Lm*. WT or p47$^{phox-/-}$ BMDCs (1×10^6), untreated or pulsed with 1×10^8 CFUs of UVi *Lm* for 5 hours, were i.v. injected into WT recipient mice. The recipients also received a booster injection, 1×10^8 CFUs of UVi *Lm* i.p., on day 14 after serum collection. **A:** Schematic timeline of adoptive transfer and serum collection. **B:** Serum titers for IgG and IgM specific for whole *Lm* were determined by ELISA. Absorbance values (Titer-1) represent the mean ± SEM. $^*P \leq 0.05$, $^{**}P \leq 0.005$, and $^{***}P \leq 0.0005$. Results are representative of two individual experiments, with five and nine of each genotype in serial experiments.

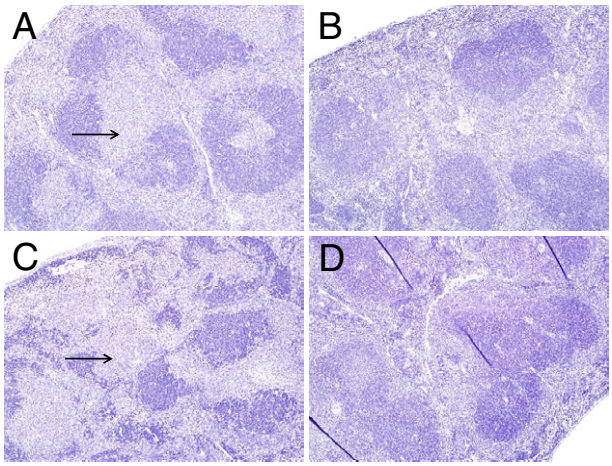

Figure 4. Histological characteristics of *Lm*-infected spleens. **A** to **D:** H&E and immunohistochemistry labeling for *Lm* in infected spleens. **A:** WT spleen, immunostaining against *Lm* 3 days after infection. Original magnification, ×8. **B:** WT spleen, mild increase in lymphocytes, 14 days after infection. Original magnification, ×8 (H&E). **C:** p47$^{phox-/-}$ spleen, immunostaining against *Lm* 14 days after infection. Original magnification, ×8 (severe inflammation with lymphoid necrosis). **D:** p47$^{phox-/-}$ spleen, diffuse inflammation with histiocytosis, 3 days after infection. Original magnification, ×8.

p47$^{phox-/-}$ and WT mice 3 and 14 days after infection revealed diffuse inflammation with histiocytosis. In p47$^{phox-/-}$ mice, splenic lesion necrosis was more severe and consisted of diffuse severe inflammation with histiocytosis (Figure 4). Thus, p47$^{phox-/-}$ mice have enhanced inflammatory cytokine secretion and extensive tissue inflammation during primary *Lm* infection.

As illustrated in Figure 5A, live *Lm* stimulated significantly enhanced anti–*Lm*-specific IgM (25-fold) and IgG (45-fold) titers in p47$^{phox-/-}$ mice on day 120 compared with similarly challenged WT mice. Interestingly, the kinetics of IgM production showed that, although both WT and p47$^{phox-/-}$ titers peaked on day 7, the anti–*Lm*-specific IgM was sustained in p47$^{phox-/-}$ mice but decreased in WT mice over time. Strikingly, the p47$^{phox-/-}$ anti-*Lm* IgG titer increased 225-fold from day 14 to 120 compared with fivefold in WT mice. Furthermore, unlike UVi *Lm*, live *Lm* infection induced 24-fold higher anti–LLO-specific IgG titers in p47$^{phox-/-}$ mice than WT mice over time (Figure 5B). Thus, live *Lm* triggers a robust anti-*Lm* and anti-LLO IgG response in p47$^{phox-/-}$ mice.

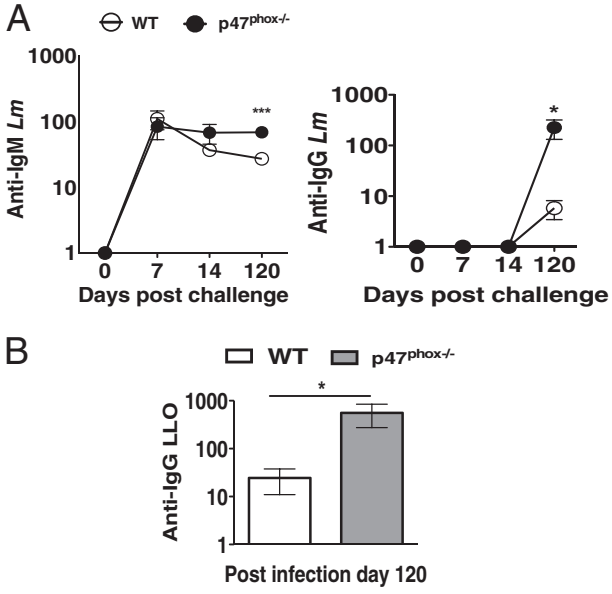

Figure 5. Ab production in response to live *Lm* challenge. Ten WT and p47$^{phox-/-}$ mice were infected i.v. with 5 × 10^4 CFUs (0.1 LD_{50}) of *Lm*. **A:** Anti-*Lm* IgM and IgG. **B:** Anti-LLO IgG-specific serum titers were determined by ELISA on the indicated days. Absorbance values (Titer-1) represent the mean ± SEM. *$P \leq 0.05$ and ***$P \leq 0.0005$.

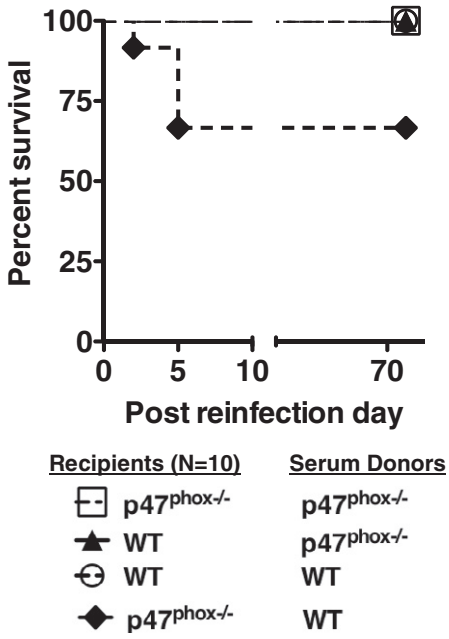

Figure 6. Serum from *Lm*-infected p47$^{phox-/-}$ mice is protective against secondary Lm challenge. Ten WT and p47$^{phox-/-}$ mice that survived primary i.v. *Lm* infection received 200 mL of pooled serum from the WT and p47$^{phox-/-}$ mice that survived *Lm* secondary reinfection, before reinfection with 10× LD_{50} of *Lm*. This figure represents survival of WT and p47$^{phox-/-}$ mice treated with pooled serum before secondary *Lm* reinfection. $P = 0.005$.

Parallel investigations in our laboratory have found that nearly 75% of p47$^{phox-/-}$ mice became moribund during the first week after *Lm* rechallenge compared with 25% of Nox2$^{-/-}$ and WT mice (Q. Liu, L. Yi, S. Sadiq-Ali, S.M. Walker, N. Zhu, and S.H. Jackson, unpublished data). Given these results and finding that both UVi and live *Lm* trigger enhanced anti-*Lm* and anti-LLO Ab production in p47$^{phox-/-}$ mice, we speculated that the observed humoral response may be protective against *Lm* in p47$^{phox-/-}$ mice. Therefore, to elucidate whether *Lm* elicited protective anti-*Lm* Ab production, we harvested immune serum from *Lm*-infected WT and p47$^{phox-/-}$ mice 6 days after *Lm* reinfection (see *Materials and Methods*) for passive Ab transfer into WT and p47$^{phox-/-}$ recipients 1 day before rechallenge with a lethal dose of *Lm*. As shown in Figure 6, all WT immune serum recipient mice survived lethal secondary *Lm* reinfection. Likewise, all of the p47$^{phox-/-}$ mice that received immune serum from secondarily reinfected p47$^{phox-/-}$ donors also survived lethal secondary *Lm* reinfection. In contrast, only 60% of the p47$^{phox-/-}$ mice that received WT immune serum samples survived lethal *Lm* secondary reinfection. These results demonstrate that, although both WT and p47$^{phox-/-}$ immune serum samples

conveyed protection against secondary *Lm* infection, only the p47$^{phox-/-}$ immune serum samples rescued both WT and p47$^{phox-/-}$ mice and are, therefore, most effective.

Discussion

We studied Ab production in p47^{phox}-deficient (p47$^{phox-/-}$) mice,[15] a murine model of CGD,[9] to examine the relative role of Nox2-dependent ROS deficiency in mediating antimicrobial humoral immunity. Similar to patients with CGD, genetically engineered murine models of the most common genetic variants of CGD each recapitulate that the phagocyte oxidase respiratory burst is critical for combating microbial infection[15,17] and that hyperinflammation is a consequence of ROS deficiency. In addition, these models allow for complex analyses of microbial-induced Nox2-dependent innate and adaptive immune responses that are not possible in humans with CGD.

Chronic disease states, such as persistent and recurrent infection in an immunodeficient host, autoimmunity, and cancer, each pose distinct tissue insults that drive chronic, and often aberrant, inflammation that is not restorative. Furthermore, the mechanisms that drive systemic inflammation during these chronic disease states are not well defined. DC- and macrophage-derived inflammatory cytokines, such as IL-6, IL-12, and TNF-α, released early after infection play a key role in innate and adaptive host defenses against both *Lm* and *Pn*.[26,27] TNF-α, IL-6, and IL-12 have also been important for protein-specific anti-*Pn* IgG production[26] and critical for T-cell–mediated *Lm* clearance.[28] *Lm*-activated APCs also stimulate CD4$^+$ and CD8$^+$ T cells to secrete interferon-γ, which further enhances macrophage bactericidal activity by preventing *Lm* escape from the phagosome[29] and by triggering macrophages to produce antimicrobial-reactive Nox2-dependent oxygen and inducible nitric oxide synthase–dependent nitrogen intermediates.[2,30] Interferon-γ also induces CD8$^+$ T cells to lyse *Lm*-infected host cells.[31,32] Consistent with previous reports[33,34] using other microorganisms and Toll-like receptor ligands, we found that p47$^{phox-/-}$ APCs are hyperresponsive to stimulation with UVi *Pn* and *Lm in vitro* and that p47$^{phox-/-}$ APC proinflammatory cytokine secretion is exaggerated compared with WT APCs. We found that the expression of selective cell surface stimulatory molecules that regulate innate and adaptive immune cell function is exaggerated in *Lm*-stimulated p47$^{phox-/-}$ APCs. In addition, our findings indicate the novel observation that *in vitro Lm*-pulsed DCs from phagocyte oxidase p47$^{phox-/-}$ mice elicit a more robust humoral immune response against *Lm* in naïve recipient mice while similarly treated WT DCs did not. Collectively, these findings indicate a role for ROS modulation of proinflammatory cellular pathways in APCs. Furthermore, the data indicate that ROS deficiency modulates an inflammatory response that to leads enhanced humoral immunity.

Although ROS are critical inflammatory mediators, interestingly, hyperinflammation is a prominent disease manifestation in phagocyte oxidase–deficient patients with CGD. In addition, hypergammaglobulinemia has been reported to be a common occurrence in patients with CGD since the first clinical description by Charles A. Janeway, Jr., M.D., and colleagues in 1954.[35,36] Notably, previous investigations of humoral immunity in murine models with reduced or change ascent to elevated Nox2 catalytic activity showed contrasting results. Richards and Clark[37] reported that phagocyte oxidase–deficient gp91^{phox}/Nox2$^{-/-}$ mice develop enhanced nonspecific IgG titers and dinitrophenyl hapten–specific anti–IgM and IgG titers. In contrast, anti–collagen-specific IgG titers were reduced in gp91^{phox}/Nox2$^{-/-}$ mice with enhanced collagen-induced arthritis.[34] Anti–collagen-specific IgG titers and collagen-induced arthritis were enhanced in *Ncf1*-mutant mice that have reduced ROS production.[38–40] Our findings demonstrate that phagocyte oxidase–deficient p47$^{phox-/-}$ mice mount a more robust humoral immune response against UVi bacteria, *Pn* and *Lm*. Furthermore, our findings demonstrate that primary and recall Ab production against *Pn* and *Lm* is enhanced in p47$^{phox-/-}$ mice.

Consistent with our findings, Dreskin et al[41] reported that patients with CGD and recently documented *Staphylococcus aureus* infection, defined as acute infection and infection within 2 years of analysis, had higher anti–*S. aureus* titers than normal controls and patients with CGD without a history of recent *S. aureus* infection. Thus, our findings implicate a role for Nox2-dependent ROS as inflammatory mediators that regulate Ab production and humoral immunity. The data also suggest that Nox2-dependent ROS influence critical processes in APC differentiation and function that attenuate proinflammatory cytokine production in combination with surface-stimulatory molecule expression, which activate Ab production.

During infection, *Lm* is absorbed by phagocytic cells and most bacteria are eliminated within phagosomes. However, occasionally, *Lm* escapes the phagosome by secreting LLO, a virulence factor that destroys the phagosomal membrane.[42] The released *Lm* then enters the cytosol, where it is able to replicate. The consequent *Lm* cytosolic invasion triggers an innate inflammatory response and induces adaptive immunity.[2,30] Although early *Lm* research[4,43] indicated that *Lm*-induced Ab production was not specific for *Lm* resistance, Edelson et al[5,6] demonstrated that antibodies against LLO provide resistance to *Lm* by neutralizing bacterial growth and pageing *Lm* escape into the cytosol. We found that IgG titers against *Lm* and LLO were significantly higher in p47$^{phox-/-}$ mice that were previously infected with *Lm* than similarly treated WT mice. In addition, we found that anti–serum samples from secondarily *Lm*-infected WT and p47$^{phox-/-}$ mice conveyed protection against *Lm* reinfection. Moreover, our findings indicate the novel observation that both WT and p47$^{phox-/-}$ recipients of serum from reinfected p47$^{phox-/-}$ mice were protected. In contrast, only 60% of p47$^{phox-/-}$ recipients of WT anti–serum samples were protected from secondary *Lm* infection. Thus, our findings indicate that, although ROS-deficient–dependent inflammation is not restorative, it can modulate an inflammatory response that is ultimately protective.

Acknowledgments

We thank Harry L. Malech and Clifford M. Snapper for careful review of the manuscript.

References

1. Zenewicz LA, Shen H: Innate and adaptive immune responses to Listeria monocytogenes: a short overview. Microbes Infect 2007, 9:1208–1215
2. Pamer EG: Immune responses to Listeria monocytogenes. Nat Rev Immunol 2004, 4:812–823
3. AlonsoDeVelasco E, Verheul AF, Verhoef J, Snippe H: Streptoccocus pneumoniae: virulance factors, pathogenesis, and vaccines. Microbiol Rev 1995, 59:591–603
4. Mackaness GB: Cellular resistance to infection. J Exp Med 1962, 116:381–406
5. Edelson BT, Cossart P, Unanue ER: Paradigm revisited: antibody provides resistance to Listeria infection. J Immun 1999, 163:4087–4090
6. Edelson BT, Unanue ER: Intracellular antibody neutralizes Listeria growth. Immunity 2001, 14:503–512
7. Bokoch GM, Knaus UG: NADPH oxidases: not just for leukocytes anymore! Trends Biochem Sci 2003, 28:502–508
8. Geiszt M, Leto TL: The Nox family of NAD(P)H oxidases: host defense and beyond. J Biol Chem 2004, 279:51715–51718
9. Heyworth PG, Cross AR, Curnutte JT: Chronic granulomatous disease. Curr Opin Immunol 2003, 15:578–584
10. Williams DA, Tao W, Yang F, Kim C, Gu Y, Mansfield P, Levine JE, Petryniak B, Derrow CW, Harris C, Jia B, Zheng Y, Ambruso DR, Lowe JB, Atkinson SJ, Dinauer MC, Boxer L: Dominant negative mutation of the hematopoietic-specific Rho GTPase, Rac2, is associated with a human phagocyte immunodeficiency. Blood 2000, 96:1646–1654
11. Ambruso DR, Knall C, Abell AN, Panepinto J, Kurkchubasche A, Thurman G, Gonzalez-Aller C, Hiester A, deBoer M, Harbeck RJ, Oyer R, Johnson GL, Roos D: Human neutrophil immunodeficiency syndrome is associated with an inhibitory Rac2 mutation. Proc Natl Acad Sci U S A 2000, 97:4654–4659
12. Matute JD, Arias AA, Wright NA, Wrobel I, Waterhouse CC, Li XJ, Marchal CC, Stull ND, Lewis DB, Steele M, Kellner JD, Yu W, Meroueh SO, Nauseef WM, Dinauer MC: A new genetic subgroup of chronic granulomatous disease with autosomal recessive mutations in p40 phox and selective defects in neutrophil NADPH oxidase activity. Blood 2009, 114:3309–3315
13. Assari T: Chronic granulomatous disease: fundamental stages in our understanding of CGD. Med Immunol 2006, 5:4
14. Rosenzweig SD: Inflammatory manifestations in chronic granulomatous disease (CGD). J Clin Immunol 2008, 28(Suppl 1):S67–S72
15. Jackson SH, Gallin JI, Holland SM: The p47phox mouse knock-out model of chronic granulomatous disease. J Exp Med 1995, 182:751–758
16. Liu Q, Cheng LI, Yi L, Zhu N, Wood A, Changpriroa CM, Ward JM, Jackson SH: p47phox deficiency induces macrophage dysfunction resulting in progressive crystalline macrophage pneumonia. Am J Pathol 2009, 174:153–163
17. Pollock JD, Williams DA, Gifford MA, Li LL, Du X, Fisherman J, Orkin SH, Doerschuk CM, Dinauer MC: Mouse model of X-linked chronic granulomatous disease, an inherited defect in phagocyte superoxide production. Nat Genet 1995, 9:202–209
18. Foulds KE, Rotte MJ, Seder RA: IL-10 is required for optimal CD8 T cell memory following Listeria monocytogenes infection. J Immunol 2006, 177:2565–2574
19. Vasilevsky S, Colino J, Puliaev R, Canaday DH, Snapper C: Macrophages pulsed with Streptococcus pneumoniae elicit a T cell-dependant antibody response upon transfer into naive mice. J Immunol 2008, 181:1787–1797
20. Zavilgesky GB, Gurzadyan GG, Nikogosyan DN: Pyrimidine dimers, single-strand breaks and crosslinks induced DNA by powerful laser UV irradiation. Photochem Photobiol 1984, 8:175–187
21. Colino J, Shen Y, Snapper CM: Dendritic cells pulsed with intact Streptococcus pneumoniae elicit both protein- and polysaccharide-specific immunoglobulin isotype responses in vivo through distinct mechanisms. J Exp Med 2002, 195:1–13
22. Bhunia AK: Antibodies to Listeria monocytogenes. Crit Rev Microbiol 1997, 23:77–107
23. Dinauer MC, Deck MB, Unanue ER: Mice lacking reduced nicotinamide adenine dinucleotide phosphate oxidase activity show increased susceptibility to early infection with Listeria monocytogenes. J Immunol 1997, 158:5581–5583
24. Shiloh MU, MacMicking JD, Nicholson S, Brause JE, Potter S, Marino M, Fang F, Dinauer M, Nathan C: Phenotype of mice and macrophages deficient in both phagocyte oxidase and inducible nitric oxide synthase. Immunity 1999, 10:29–38
25. Endres R, Luz A, Schulze H, Neubauer H, Futterer A, Holland SM, Wagner H, Pfeffer K: Listeriosis in p47(phox-/-) and TRp55-/- mice: protection despite absence of ROI and susceptibility despite presence of RNI. Immunity 1997, 7:419–432
26. Khan AQ, Shen Y, Wu Z-Q, Wynn TA, Snapper CM: Endogenous pro- and anti-inflammatory cytokines differentially regulate an in vivo humoral response to Streptococcus pneumoniae. Infect Immun 2002, 70:749–761
27. Tam MA, Wick MJ: Dendritic cells and immunity to Listeria: tipDCs are a new recruit. Trends Immunol 2004, 25:335–339
28. Nakane A, Numata A, Minagawa T: Endogenous tumor necrosis factor, interleukin-6, and gamma interferon levels during Listeria monocytogenes infection in mice. Infect Immun 1992, 60:523–528
29. Portnoy DA, Schreiber RD, Connely P, Tilney LG: Gamma interferon limits access of Listeria monocytogenes to the macrophage cytoplasm. J Exp Med 1989, 170:2141–2146
30. Shaughnessy LM, Swanson JA: The role of the activated macrophage in clearing Listeria monocytogenes infection. Front Biosci 2007, 12: 2683–2692
31. Gregory SH, Liu CC: CD8+ T-cell-mediated response to Listeria monocytogenes taken up in the liver and replicating within hepatocytes. Immunol Rev 2000, 174:112–122
32. Jiang X, Gregory SH, Wing EJ: Immune CD8+ T lymphocytes lyse Listeria monocytogenes-infected hepatocytes by a classical MHC class I-restricted mechanism. J Immunol 1997, 158:287–293
33. Brown KL, Bylund J, MacDonald KL, Song-Zhao GX, Elliott MR, Falsafi R, Hancock RE, Speert DP: ROS-deficient monocytes have aberrant gene expression that correlates with inflammatory disorders of chronic granulomatous disease. Clin Immunol 2008, 129:90–102
34. George-Chandy A, Nordstrom I, Nygren E, Jonsson IM, Postigo J, Collins LV, Eriksson K: Th17 development and autoimmune arthritis in the absence of reactive oxygen species. Eur J Immunol 2008, 38: 1118–1126
35. Carnide EG, Jacob CA, Castro AM, Pastorino AC: Clinical and laboratory aspects of chronic granulomatous disease in description of eighteen patients. Pediatr Allergy Immunol 2005, 16:5–9
36. Bridges RA, Berendes H, Good RA: A fatal granulomatous disease of childhood: the clinical, pathological, and laboratory features of a new syndrome. AMA J Dis Child 1959, 97:387–408
37. Richards SM, Clark EA: BCR-induced superoxide negatively regulates B-cell proliferation and T-cell-independent type 2 Ab responses. Eur J Immunol 2009, 39:3395–3403
38. Hultqvist M, Olofsson P, Holmberg J, Backstrom BT, Tordsson J, Holmdahl R: Enhanced autoimmunity, arthritis, and encephalomyelitis in mice with a reduced oxidative burst due to a mutation in the Ncf1 gene. Proc Natl Acad Sci U S A 2004, 101:12646–12651
39. Hultqvist M, Backlund J, Bauer K, Gelderman KA, Holmdahl R: Lack of reactive oxygen species breaks T cell tolerance to collagen type II and allows development of arthritis in mice. J Immunol 2007, 179:1431–1437
40. Hagenow K, Gelderman KA, Hultqvist M, Merky P, Backlund J, Frey O, Kamradt T, Holmdahl R: Ncf1-associated reduced oxidative burst promotes IL-33R+ T cell-mediated adjuvant-free arthritis in mice. J Immunol 2009, 183:874–881
41. Dreskin SC, Goldsmith PK, Gallin JI: Immunoglobulins in the hyper-immunoglobulin E and recurrent infection (Job's) syndrome: deficiency of anti-Staphylococcus aureus immunoglobulin A. J Clin Invest 1985, 75:26–34
42. Bielecki J, Youngman P, Connelly P, Portnoy DA: Bacillus subtilis expressing a haemolysin gene from Listeria monocytogenes can grow in mammalian cells. Nature 1990, 345:175–176
43. Osebold JW, Sawyer MT: Immunization studies on listeriosis in mice. J Immunol 1957, 78:262–268